Polymerization shrinkage kinetics andshrinkage-stress in dental resin-composites

DOI:
10.1016/j.dental.2016.05.006

Document Version
Accepted author manuscript

DENTAL MATERIALS XXX (2016) XXX–XXX

Available online at www.sciencedirect.com

ScienceDirect

journal homepage: www.intl.elsevierhealth.com/journals/dema

Polymerization shrinkage kinetics and shrinkage-stress in dental resin-composites

Hanan Al Sunbul[a,b], Nick Silikas[a,*], David C. Watts[a,c]

[a] Biomaterials Science Research Group, School of Dentistry, University of Manchester, United Kingdom
[b] College of Dentistry, King Saud University, Riyadh, Saudi Arabia
[c] Photon Science Institute, University of Manchester, United Kingdom

ARTICLE INFO

Article history:
Received 10 September 2015
Received in revised form
11 May 2016
Accepted 13 May 2016
Available online xxx

Keywords:
Resin-composite
Shrinkage-strain
Shrinkage-stress
Strain rate
Modulus of elasticity
Bulk-fill

ABSTRACT

Objectives. To investigate a set of resin-composites and the effect of their composition on polymerization shrinkage strain and strain kinetics, shrinkage stress and the apparent elastic modulus.

Methods. Eighteen commercially available resin-composites were investigated. Three specimens ($n = 3$) were made per material and light-cured with an LED unit (1200 mW/cm^2) for 20 s. The bonded-disk method was used to measure the shrinkage strain and Bioman shrinkage stress instrument was used to measure shrinkage stress. The shrinkage strain kinetics at 23 °C was monitored for 60 min. Maximum strain and stress was evaluated at 60 min. The shrinkage strain rate was calculated using numerical differentiation.

Results. The shrinkage strain values ranged from 1.83 (0.09) % for Tetric Evoceram (TEC) to 4.68 (0.04) % for Beautifil flow plus (BFP). The shrinkage strain rate ranged from 0.11 (0.01%s^{-1}) for Gaenial posterior (GA-P) to 0.59 (0.07) %s^{-1} for BFP. Shrinkage stress values ranged from 3.94 (0.40) MPa for TET to 10.45 (0.41) MPa for BFP. The apparent elastic modulus ranged from 153.56 (18.7) MPa for Ever X posterior (EVX) to 277.34 (25.5) MPa for Grandio SO heavy flow (GSO).

Significance. The nature of the monomer system determines the amount of the bulk contraction that occurs during polymerization and the resultant stress. Higher values of shrinkage strain and stress were demonstrated by the investigated flowable materials. The bulk-fill materials showed comparable result when compared to the traditional resin-composites.

1. Introduction

Polymerization shrinkage of resin-composite occurs due to the conversion of the monomer molecules in to polymer structure which is accomplished by replacing the van der waals spaces by covalent bonds and consequently reducing the free volume [1,2]. Despite the numerous advances in improving the bonding mechanism between the tooth structure and the resin-composite material, the failure of the bonding interface remains [2,3]. The defects that develop in the interfacial bonding are due to the polymerization stresses generated during the restorative placement procedure and later due to the functional thermal and mechanical stresses [4,5]. With the introduction of the bulk-fill group of materials the effect of

* *Corresponding author at*: School of Dentistry, The University of Manchester, Manchester M13 9PL, United Kingdom. Tel.: +44 1612756747.
E-mail address: nick.silikas@manchester.ac.uk (N. Silikas).

http://dx.doi.org/10.1016/j.dental.2016.05.006
0109-5641/

polymerization shrinkage is highlighted as these materials are recommended to be placed in 4 mm increments.

Several studies demonstrated the direct relationship between the stress generated during polymerization and the integrity of the restoration-tooth margins [6,7]. The polymerization process is accompanied by volumetric shrinkage of the material and its magnitude depends on the composition of the material [8,9]. The amount of the polymerization stress generated is the product of many controlling factors including the C-factor, the compliance of the dental substrate and the material properties [4,10–12].

The viscoelastic behavior of the material has an important role in the capacity of the material to flow during early stages of polymerization and on the elastic modulus development. Viscoelastic behavior of the material is another important factor that affects the polymerization stress development [5]. The viscoelasticity of the material and the volumetric shrinkage are both controlled by similar factors that make it difficult to isolate their effect on the polymerization shrinkage stress development [13,14]. In addition, the stress development is affected by the reaction kinetics as a higher polymerization rate is accompanied by high polymerization stress [15,16]. The material plastic deformation is time dependent phenomenon in which the material needs time to flow to accommodate the contraction stresses before the development of the modulus of elasticity [17–20].

Different methods have been proposed to reduce polymerization shrinkage and its resultant stress. These methods include incremental placement of the restoration, soft start curing technique, the use of stress absorbing cavity liners and modification in the material composition [2,21,22]. Polymerization shrinkage for monomers such as Bis-GMA and TEGDMA had been found to be substantially higher than the typically filled composites [13,23]. There is a direct relation between the increase in filler loading and the reduction in polymerization shrinkage [24–26]. The incorporation of pre-polymerized resin fillers (organic fillers) decreases the volume fraction of the polymerizable resin and increases the filler volume fraction resulting in reduction of the polymerization shrinkage. Flowable (low-viscosity) resin-composites have been reported with higher polymerization shrinkage as a result of reduced filler loading [13,27]. Nano-composites are a class of composite that was introduced for its improved mechanical properties, esthetic outcomes and reduced polymerization shrinkage [28–31].

Several modifications have been made to the monomer systems of resin-composite materials to reduce the polymerization shrinkage. Many low shrinkage resin-composites have been commercially introduced to the market. Among these is the introduction of a high molecular based monomer with initially low double bond concentration (Dimer acid based monomer) an example of these materials is N'Durance from Septodont, France. It demonstrated lower polymerization shrinkage and higher degree of conversion when compared with conventional monomers as Bis-GMA and UDMA [32].

SDR® bulk-fill material has been introduced with modified UDMA by introducing photo-active groups to the monomer. It has been shown that this material resulted in lower shrinkage stress compared to other flowable and conventional composites [33]. TCD-DI-HEA was also introduced as a low shrinking monomer and it was incorporated in Venus diamond material from Haeraus Kulzer GmbH, Germany. This low viscosity monomer has a rigid back bone that results in low shrinking behavior [22,34,35]. In addition, ethoxylated bisphenol A dimethacrylate (Bis-EMA) which is a Bis-GMA analog with lower viscosity due to the absence of hydroxyl groups from its structure was introduced for a similar purpose. It has been found to provide lower polymerization shrinkage when combined with other conventional monomers such as UDMA and Bis-GMA [36].

In this study eighteen commercially available materials from different classes were investigated for their shrinkage strain, shrinkage stain kinetics, stress and modulus of elasticity. The null hypothesis was that there are no significant differences in the results between the bulk-fill materials and the other investigated materials.

2. Materials and methods

Eighteen commercially available resin-composites with different viscosities were investigated. The materials represented a wide range of dental applications. Materials' details and manufacturers' specifications are shown in Table 1.

2.1. *Shrinkage strain measurement*

The 'bonded-disk' method described by Watts and Marouf in 2000 was used to determine shrinkage-strain [37]. Resin-composite paste specimens of circular disk geometry were prepared within 15 mm diameter brass rings of square cross section fixed on a 3.0 mm thick glass slab. The upper surface of the glass slab was lightly grit-blasted with alumina powder to promote bonding of the composite to the glass surface. The specimen was 1.0 mm in height and 8 mm in width. The disks were positioned centrally within the brass rings, leaving a free space around the disk. A flexible 22 mm × 22 mm size and 0.1 mm thick glass cover slip (VWR International Ltd., borosilicate glass, thickness No.0) was placed in close contact above the specimen, supported laterally by the brass ring. A glass plate was used during the preparation of the specimens, in conjunction with the cover slips, to compress the composite pastes into circular disks. Resin-composite specimens of circular disk geometry were of 0.12 g to obtain the required diameter of 8 mm. This value was obtained through pilot testing of different resin-composite weights and direct measurement of the resultant disk.

The bonded-disk arrangement is placed upon a custom jig. The jig was made of an aluminum stand with a horizontal 'stage' for specimen placement with two stainless steel clips to hold the glass slab. Mounted into the stage was a brass ring. The brass ring had a hollow center of 10 mm diameter through which the tip of a light curing unit was fixed in place. A clamp arrangement was attached to the stage to hold the uni-axial LVDT (linear variable displacement transducer) measuring system and allowed for vertical adjustment of its position. The LVDT measuring system, of 8 g active mass, was positioned centrally onto the cover slip. Specimens were light-cured by 20 s direct irradiation from beneath the glass slab at 1200 mW/cm^2 using an Elipar S10 LED curing light from

Please cite this article in press as: Al Sunbul H, et al. Polymerization shrinkage kinetics and shrinkage-stress in dental resin-composites. Dent Mater (2016), http://dx.doi.org/10.1016/j.dental.2016.05.006

Table 1 – Materials details and manufacturer' specifications.

Material	Filler loading (vol.%)	Resin matrix	Manufacturer	Type
Gradia direct posterior (GDP)	65	UDMA, DM	GC Corporation, Tokyo, Japan	Micro-hybrid conventional
G-aenial posterior (GA-P)	65	UDMA, dimethacrylate	GC Corporation, Tokyo, Japan	Micro-hybrid conventional
G-aenial anterior (GA-A)	63	UDMA, dimethacrylate	GC Corporation, Tokyo, Japan	Micro-hybrid conventional
G-aenial universal flow (GA-F)	50	UDMA Bis-MePP, TEGMA	GC Corporation, Tokyo, Japan	Nano-hybrid flowable
Ever X posterior (EVX)	57	Bis-GMA, TEGDMA, PMMA	GC Corporation, Tokyo, Japan	Fiber reinforced Packable BF
Venus diamond (VD)	64	TCD-DI-HEA, UDMA	Heraeus Kulzer GmbH, Germany	Nano-hybrid conventional
Venus bulk fill (V-BF)	38	UDMA, BIS-EMA	Heraeus Kulzer GmbH, Germany	Nano-hybrid flowable BF
Tetric Evoceram (TEC)	53–55	Bis-GMA, UDMA, BIS-EMA	Ivoclar Vivadent, Schaan, Liechtenstein	Nano-hybrid conventional
Tetric Evoceram bulk fill (TEC-BF)	60–61	Bis-GMA, UDMA, BIS-EMA	Ivoclar Vivadent, Schaan, Liechtenstein	Nano-hybrid Packable BF
Smart dentin replacement (SDR®)	44	Modified UDMA, BIS-EMA, TEGDMA	Dentsply Caulk, Milford, Delaware, USA	Fluoride-containing flowable BF
Spectrum TPH (STPH)	57	BisGMA, Bis-EMA & TEGDMA	Dentsply Caulk, Milford, Delaware, USA	Micro-hybrid conventional
Filtek supreme XTE (FSE)	55.6	BisGMA, Bis-EMA, UDMA, TEGDMA, PEGDMA	3M ESPE, USA	Nano-hybrid flowable
Estelite flow quick (EFQ)	53	Bis-MPEPP, TEGDM, UDMA	Tokuyama Dental Corporation, Tokyo, Japan	Micro-hybrid flowable
Beautifil flow plus (BFP)	47	Bis-GMA, TEGDM	Shofu INC, Japan	Nano-hybrid Fluoride-containing Flowable
Grandio SO heavy flow (GSO)	68	Bis-GMA, Bis-EMA, TEGDMA	Voco, Cuxhaven, Germany	Nano-hybrid flowable
X-tra base (XB)	58	MMA, Bis-EMA	Voco, Cuxhaven, Germany	Hybrid flowable BF
N'Durance (ND)	65	Bis-GMA, UDMA, DDCDMA	Septodont, France	Nano-hybrid packable
Premise (PR)	69	BIS-EMA, TEGDMA	Kerr Corporation, Orange, USA	Nano-hybrid conventional

3M ESPE, and at an initial room temperature of $23 \pm 1\,^{\circ}C$. The light output was measured using a laboratory grade NIST-referenced USB-4000 spectrometer (MARC Resin Calibrator v.3, Blue-light analytics Inc, Halifax, NS, Canada). The measurements were made continuously every second for 60 min from irradiation time.

Three specimens were made for each material. The signal from the LVDT was transmitted to a computer by a signal conditioning unit (E 309, RDP Electronics Ltd., Wolverhampton, UK) and a high resolution analog to digital converter and data logger (PICO ADC-20 Data logger, Pico Technology Ltd, Cambs., UK). Following mechanical equilibration, data were captured for 60 min from 20 s prior to commencement of irradiation with sampling every second.

The data were then processed using SigmaPlot (SigmaPlot 2008 ver. 11, SPSS Inc., IL, USA). Using the following equation (Eq. (1)) the strain values were calculated. For each composite the maximum recorded shrinkage strain of each of the three runs was recorded and the mean and standard deviation were calculated. In which ε is the strain, ΔL is the change in length and L_0 is the original length.

$$\varepsilon = \frac{\Delta L}{L_0} \tag{1}$$

2.2. *Shrinkage stress measurement*

Shrinkage-stress was measured using The *Bioman* shrinkage-stress instrument that was designed and constructed at the University of Manchester [38]. Components were bolted to a 2 cm thick stainless steel base-plate. Support frame was used to vertically mount the components of the instrument.

Please cite this article in press as: Al Sunbul H, et al. Polymerization shrinkage kinetics and shrinkage-stress in dental resin-composites. Dent Mater (2016), http://dx.doi.org/10.1016/j.dental.2016.05.006

A cantilever load-cell of 500 kg capacity was fitted with a rigid integral clamp at the compliant end (the free end) of the cantilever to securely hold a circular steel rod with 10 mm diameter and 22 mm long vertically and perpendicular to the load-cell axis. The bottom of the rod was sand-blasted to aid in composite retention and formed the top surface of the specimen chamber. The lower surface of the specimen chamber is made by a 3 mm thick glass plate that was also sand blasted for the same purpose. The glass plate was held rigidly with special clamp during the measurements. The specimen chamber gap was set with the aid of a feeler gauge to 0.8 mm giving a configuration-factor of 6.25 according to the following equation where d and h are the diameter and thickness of the disk specimen (Eq. (2))

$$C = \frac{d}{2h} \tag{2}$$

The specimen was irradiated from the bottom surface through the glass plate for 20 s at 1200 mW/cm^2 using an Elipar S10 LED curing light from 3M ESPE, and at an initial room temperature of 23 ± 1 °C. During polymerization, the stresses produced within the specimen caused a slight displacement of the free end of the load-cell. The load-signal from the cantilever cell was amplified by a wide-range strain indicator (Model 3800, Vishay, Measurements Group, Rayleigh, NC, USA). The signals produced by the displacement were continually sent to a computer via a signal conditioning unit and a high resolution analog to digital converter and data logger (ADC-20 multi-channel data acquisition unit and PicoLog software; Picotech, Cambridge, UK).

Three specimens were made from each material. The material required to make 0.8 mm thickness specimen of 10 mm diameter was 0.14 g that was determined by pilot mass testing and direct measurement of the disks. The unset material was placed on the glass plate which was then positioned and stabilized by the adjustment screw. The material then was pressed between the glass slab and the steel rod and left for one minute to allow relaxation of any internal stresses produced during manipulation. Data were recorded for 60 min from 20 s prior to commencement of irradiation, with sampling each second.

The data were then processed using SigmaPlot (SigmaPlot 2008 ver. 11, SPSS Inc., IL, USA). The stress value in MPa is then obtained from the recorded load divided by the specimen disk area. For each material the maximum recorded shrinkage stress of each of the three runs was recorded and the mean and standard deviation were calculated.

$$\sigma = \frac{\text{Force}}{\text{Area}} \tag{3}$$

The shrinkage strain rate was calculated by numerical differentiation of the shrinkage strain data with respect to time. This was made for the first 200 s of the data from the three runs, using MATLAB (ver. 7.6, MathWorks Inc., MI, USA).

The modulus of elasticity was calculated from the measured polymerization shrinkage strain (ε) and stress (σ) following Eq. (4).

$$E = \frac{\sigma}{\varepsilon} \tag{4}$$

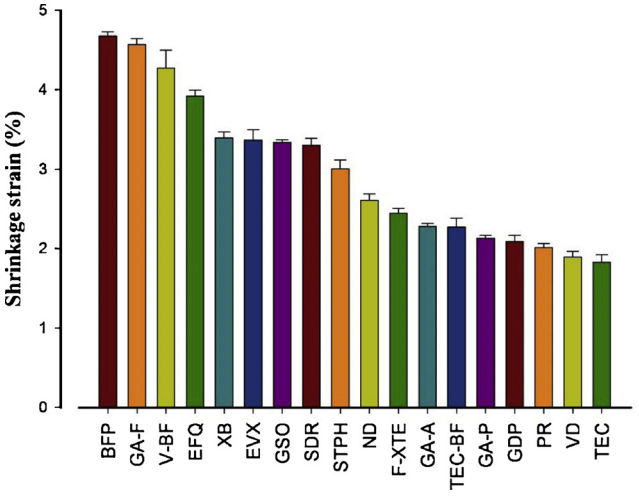

Fig. 1 – Shrinkage strain means and standard deviations of the investigated materials.

2.3. *Statistical analysis*

A statistical package (SPSS ver. 16.0, SPSS Inc., IL, USA) was used to analyze the data. The shrinkage strain, shrinkage strain rate, shrinkage stress and modulus of elasticity results were analyzed using one-way ANOVA. Data were tested for equal variances using the homogeneity test ($p < 0.05$). Equal variances were assumed, thus multiple comparisons using a Tukey post hoc test were conducted to establish homogenous subsets. Linear regression analyzes were made to correlate the measured properties.

3. Results

The results of the studied materials are summarized as means and standard deviations in Table 2. The results are graphically shown in Figs. 1–4. The shrinkage strain values ranged from 1.83% (TEC) to 4.68% (BFP). The values for the bulk-fill composites ranged from 2.27% (TEC-BF) to 4.27% (V-BF). The

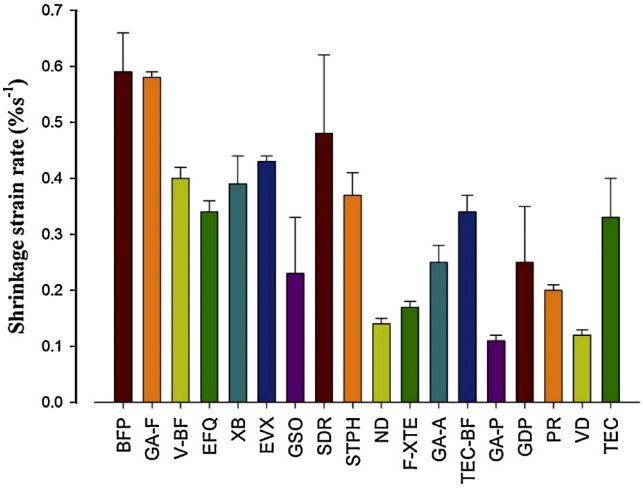

Fig. 2 – Shrinkage strain rate means and standard deviations of the investigated materials.

Table 2 – Shrinkage strain and strain rate, shrinkage stress and the apparent modulus of elasticity mean values and standard deviations.

Material	Shrinkage strain (%)	Maximum shrinkage Strain rate (%s^{-1})	Shrinkage stress (MPa)	Apparent modulus of elasticity-E (MPa)
GDP	2.09^{a,b,c}	0.25^{a,b,c,d}	5.21^{a,b,c,d,e}	250.40^{a,b}
	(0.08)	(0.10)	(0.15)	(15.9)
GA-P	2.13^{b,c}	0.11^{e}	5.17^{a,b,c,d}	242.78^{a,b,c}
	(0.04)	(0.01)	(0.17)	(9.7)
GA-A	2.28^{c,d}	0.25^{a,b,c,d}	5.13^{a,b,c,d}	225.20^{b,c,d}
	(0.04)	(0.03)	(0.06)	(2.9)
GA-F	4.5^{g,h}	0.5^{g,h}	9.08^{h}	198.94^{c,d,e,f}
	(0.08)	(0.01)	(0.55)	(13.9)
EVX	3.36^{f}	0.43^{f,g}	5.16^{a,b,c,d}	153.56^{f}
	(0.13)	(0.01)	(0.68)	(18.7)
VD	1.89^{a,b}	0.12^{a,e}	4.65^{a,b,c}	246.27^{a,b,c}
	(0.07)	(0.01)	(0.20)	(2.13)
V-BF	4.2^{g}	0.40^{f}	6.62^{e,f,g}	154.95^{f}
	(0.23)	(0.02)	(0.63)	(11.0)
TEC	1.83^{a}	0.33^{b,c,d,f}	3.94^{a}	216.41^{b,c,d,e}
	(0.09)	(0.07)	(0.40)	(31.8)
TEC-BF	2.27^{c,d}	0.34^{b,c,d,f}	4.1^{a,b}	181.24^{d,e,f}
	(0.11)	(0.03)	(0.26)	(20.3)
SDR®	3.30^{f}	0.48^{f,g,h}	5.48^{b,c,d,e}	166.25^{e,f}
	(0.09)	(0.14)	(0.05)	(5.3)
STPH	3.00	0.37^{d,f}	7.20^{f,g}	239.74^{a,b,c}
	(0.11)	(0.04)	(0.41)	(11.2)
F-XTE	2.44^{d,e}	0.17^{a,e}	5.79^{c,d,e,f}	237.13^{a,b,c}
	(0.06)	(0.01)	(0.26)	(9.3)
EFQ	3.92	0.34^{c,d,f}	10.19^{h}	260.3^{a,b}
	(0.08)	(0.02)	(0.87)	(21.5)
BFP	4.6^{h}	0.5^{h}	10.45^{h}	223.55^{b,c,d}
	(0.04)	(0.07)	(0.41)	(9.0)
GSO	3.34^{f}	0.23^{a,b,c,e}	9.40^{h}	277.34^{a}
	(0.03)	(0.01)	(0.85)	(25.5)
XB	3.39^{f}	0.39^{d,f}	7.21^{g}	212.40^{b,c,d,e}
	(0.07)	(0.05)	(0.13)	(2.8)
ND	2.61^{e}	0.14^{a,e}	6.48^{d,e,f,g}	249.44^{a,b,c}
	(0.08)	(0.01)	(0.57)	(28.9)
PR	2.01^{a,b,c}	0.20^{a,b,e}	5.19^{a,b,c,d}	257.67^{a,b}
	(0.05)	(0.01)	(0.29)	(14.6)

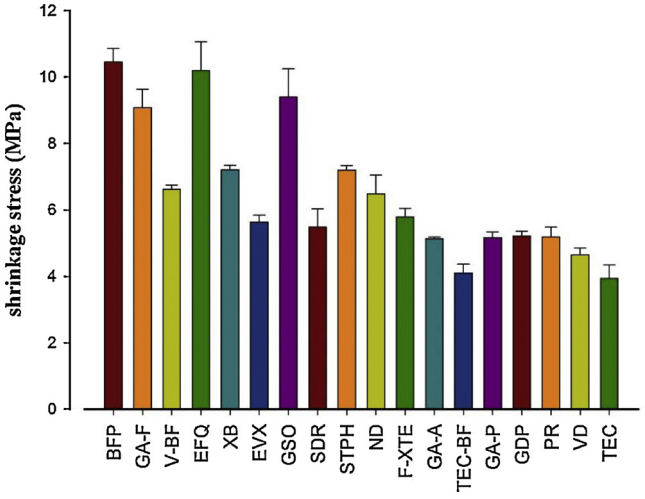

Fig. 3 – Shrinkage stress means and standard deviations of the investigated materials.

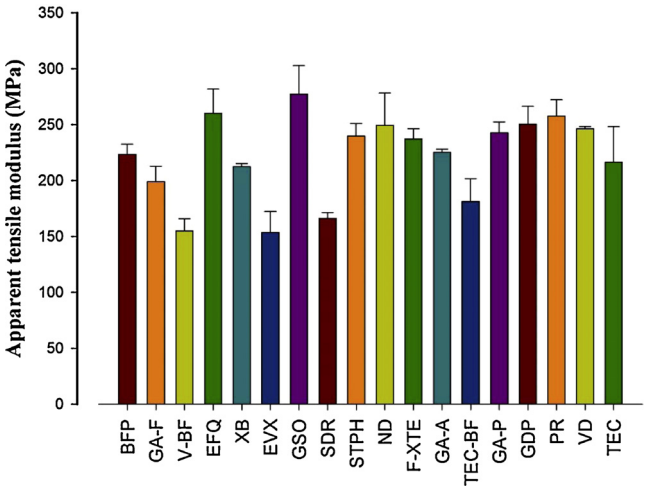

Fig. 4 – Apparent modulus of elasticity means and standard deviations of the investigated materials.

Please cite this article in press as: Al Sunbul H, et al. Polymerization shrinkage kinetics and shrinkage-stress in dental resin-composites. Dent Mater (2016), http://dx.doi.org/10.1016/j.dental.2016.05.006

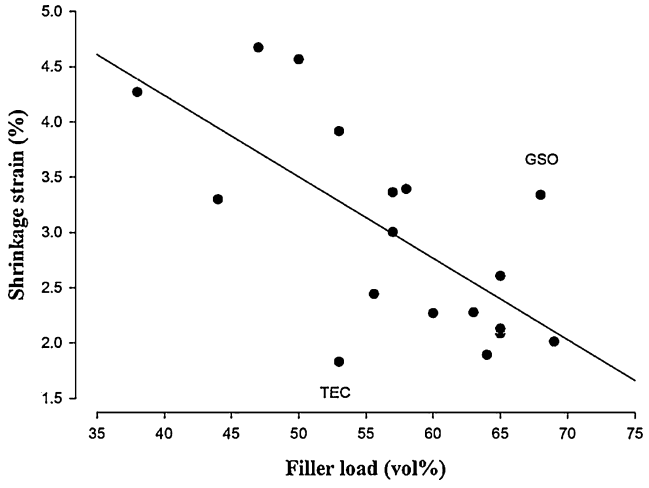

Fig. 5 – Linear regression analysis of the shrinkage strain and filler lading ($r^2 = 0.68$).

shrinkage strain rate ranged from 0.11%s^{-1} (GA-P) to 0.59%s^{-1} (BFP).

The polymerization shrinkage stress ranged from 3.94 MPa (TEC) to 10.45 MPa (BFP). For the bulk-fil materials the stress ranged from 5.16 MPa (EVX) to 7.21 MPa (XB). For the apparent modulus of elasticity the values ranged from 153.56 MPa (EVX) to 277.34MPA (GSO).

Regression analysis revealed a correlation value between the shrinkage strain and the filler loading of $r^2 = 0.46$ and $r^2 = 0.68$ after excluding the outliers (TEC and GSO) as in Fig. 5. Polymerization strain had a good correlation to polymerization stress ($r^2 = 0.68$) as in Fig. 6. The correlation between the polymerization stress and shrinkage rate was $r^2 = 0.21$. The correlation between the elastic modulus and the filler loading was found to be 0.46 and it increased up to 0.57 by excluding the outlier (EVX) Fig. 7. There was no correlation between the polymerization strain and the modulus of elasticity and between the polymerization stress and the modulus of elasticity ($r^2 = 0.18$ and 0.05 respectively).

4. Discussion

The null hypothesis was rejected as the bulk-fill materials results were within the same range as those of the other investigated materials. In the polymerization strain results TEC-BF was within the materials that showed lower shrinkage strain values (2.27%). In the polymerization strain rate results, the flowable bulk-fill SDR material had a high rate of 0.48%s^{-1} which was not significantly different from the highest rate measured with the flowable BFP (0.59%s^{-1}). Polymerization stress results for the material TEC-BF (4.10 MPa) was not significantly different from TEC which gave the lowest stress values (3.94 MPa) among the investigated materials. Similar results were found by other researchers [39]. Modulus of elasticity values for all bulk-fill materials were among the lower range compared to the other materials.

In this study the measurements were made for 60 min as it was proven by many researchers that 90% of the polymerization shrinkage occurs within the first hour after curing [40–42]. The magnitude of the shrinkage of the material is controlled by the material composition while the amount of stress generated from the shrinkage is dependent on the cavity configuration and compliance, material composition and the viscoelastic nature of the material [1,13,43,44]. The rate of polymerization has been found to influence the amount of stress generated from polymerization as the higher rate of polymerization results in higher stress [15,16]. In addition, the elastic modulus of the material plays an important role in the generation of stress during polymerization. As the material continues to polymerize the modulus of elasticity starts to develop and generates stresses within the material [44–46].

The linear regression analysis between the shrinkage strain values and filler loading of the investigated materials showed $r^2 = 0.46$ (Fig. 5). This correlation is more toward moderate negative correlation and it is noteworthy that by excluding GSO and TEC the correlation increased to $r^2 = 0.68$. Despite being one of the most heavily filled materials, GSO gave a shrinkage strain value of 3.34% which showed no significant difference compared to the medium filled material XB (3.39). On the other

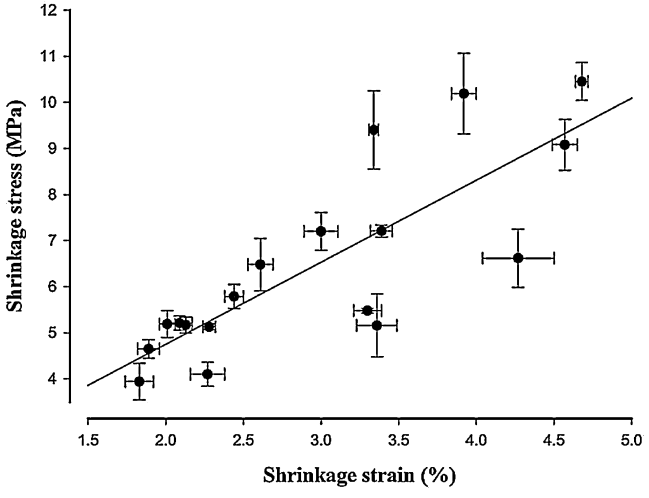

Fig. 6 – Linear regression analysis of the shrinkage stress and shrinkage strain ($r^2 = 0.66$).

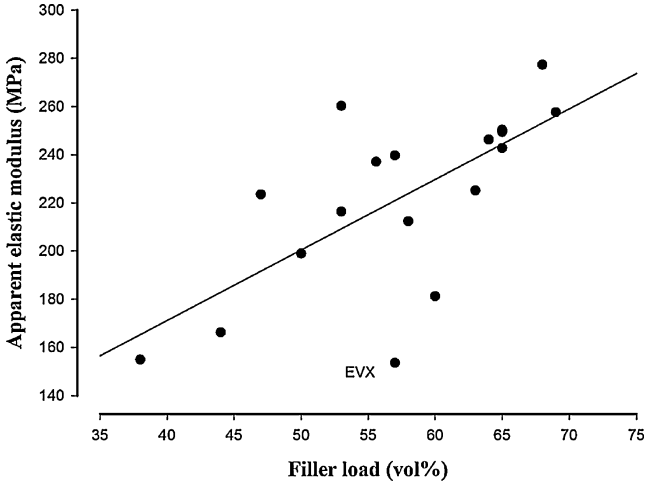

Fig. 7 – Linear regression analysis of the apparent elastic modulus and filler loading ($r^2 = 0.57$).

Please cite this article in press as: Al Sunbul H, et al. Polymerization shrinkage kinetics and shrinkage-stress in dental resin-composites. Dent Mater (2016), http://dx.doi.org/10.1016/j.dental.2016.05.006

hand TEC showed a low shrinkage strain value that is comparable to the heavily filled materials such as PR, VD and GDP. A possible explanation could be the differences in the conversion level of these materials. The close relationship between the degree of conversion and the shrinkage makes all the parameter that controls the degree of conversion affect the shrinkage such as the monomer reactivity and the network formation [47,48]. GSO is nano-hybrid flowable material that contains TEGDMA in its monomer system. Despite the high filler loading, the high reactivity of these monomers causes high conversion level and therefore high shrinkage [42,49].

TEC is a low shrinking nano-hybrid material that showed the lowest shrinkage strain values, similar to the heavily filled materials in this study. This could be explained by the monomer system that is composed of Bis-GMA and UDMA. Comparing these monomers to TEGDMA, which is present in the other flowable materials, TEGDMA is known to have higher reactivity and will lead to higher double bond conversion and subsequently more shrinkage [20,42,50].

Shrinkage strain and shrinkage stress had a good correlation (Fig. 6). This clearly shows that as the amount of shrinkage increases the stress generated will increase subsequently. BFP showed the highest strain and stress among the investigated material and on the other hand TEC showed the least strain and stress among the materials. BFP is a flowable material based on Bis-GMA and TEGDMA. As it was previously mentioned, TEGDMA has high reactivity and smaller molecular size which means high double bond concentration resulting into more volume loss after curing of the material [51]. This result was in agreement with others in which it was found that that the viscoelastic properties play an important role in stress development in addition to the monomer properties of the material [2,13,52–54].

Although there was a weak correlation between the shrinkage strain rate and the stress, positive association was seen. This could be due to the wide range of material tested from different groups which makes it difficult to isolate the effect of the polymerization rate on the stress generation. Several factors contribute to the amount of stress generation besides the polymerization kinetics, including the conversion kinetics which is closely affected by the material chemical composition [20,38,55–57]. Moreover, some materials develop elastic modulus at a low conversion which means that even at a low reaction rate there is no further plastic deformation and the stress starts to build up [18,20,58]. This can be clearly demonstrated by the high stress values of EFQ and GSO compared to their low polymerization strain rate.

In this study the modulus of elasticity was calculated using the measured stress and strain by applying the equation specified in the methodology (Eq. (4)). Stress–strain behavior of the material can be used to describe the relative stiffness of the material and is represented as a modulus of elasticity. Modulus of elasticity is an important parameter for the clinical success of dental restorations. Dental restorative materials are required to have elastic modulus that can withstand the masticatory forces and to be comparable to that of the tooth structure [59–61]. The elastic modulus at 60 min after curing was calculated and studied. The values of the present results are low compared to the experimentally measured elastic modulus of previous studies [62,63]. The possible explanation could be that the material thickness was low in the strain measurement therefore the resultant shrinkage was low. On the other hand, the stress generated during measurement is dependent on the compliance of the measurement set-up as the material was bonded to the steel rod from the top and the glass slide from the bottom.

The elastic modulus showed a positive correlation to the filler loading (with an exception to EVX) which is in agreement with many studies [64–66]. The fiber reinforced EVX material showed a lower elastic modulus despite their filler loading of (57%) compared to the other lower filled as V-BF and SDR. The major difference in this material is the nature of its filler system which is based on short glass fibers. Glass fibers were added for the purpose of improving the strength of the material and prevention of crack propagation [67,68]. On the contrary, in this study EVX showed the lowest elastic modulus compared to the other tested materials. The impact of the fiber reinforcement depends on the quality, quantity and adhesion of the fibers to the polymer matrix [68–70]. It is noteworthy that filler loading correlations in this study were made based on manufacturer values. Correlations based on measured filler loading might be different compared to the manufacturer values.

Despite being a flowable material, nano-hybrid GSO showed the highest elastic modulus and not significantly different from the other non-flowable materials. This result was also found by other researchers and can be explained by the high fraction of inorganic filler which will become interlocked in the resin matrix after curing. Thus, the bulk physical properties of the material will approach the properties of the filler system in the material which will lead to higher elastic modulus [63,71,72].

The polymerization stress has been found to depend on the elastic modulus. Many studies have found that the rigidity of the material has an effect on the stress produced as a result of polymerization. In addition, the elastic modulus was found to negatively relate to the polymerization strain [13,27,73–75]. Interestingly, in this study there was no correlation between the elastic modulus and the polymerization strain and polymerization stress. The results can be explained on the ground of the differences in degree of conversion levels as some materials with high degree of conversion may show a high elastic modulus. On the contrary the material with low degree of conversion or alternatively has inherently low shrinking monomer system and more flexibility may show low elastic modulus [13]. These results are more pronounced with BFP, GA-F and GSO materials. BFP is among the materials with lower filler loading that resulted in high strain and high modulus this may be explained by the presence of hydrogen bonds formed between its co-polymers (Bis-GMA and TEGDMA) [76].

The presence of TEGDMA in GA-F and GSO could explain the elastic modulus values in which the increase in the amount of the hydrogen bonds made the materials less fixable [76]. The stress results seem to follow the same pattern of the modulus of elasticity despite the lack of correlation [75]. The differences in the material behavior with the regard to the polymerization strain, polymerization kinetics, polymerization stress and modulus of elasticity could be explained by the fact that the differences in the monomer system is covered up by many other differences in the material composition

Please cite this article in press as: Al Sunbul H, et al. Polymerization shrinkage kinetics and shrinkage-stress in dental resin-composites. Dent Mater (2016), http://dx.doi.org/10.1016/j.dental.2016.05.006

such as the filler amount and type, initiator, silanization. However, this does not indicate the insignificance of the monomer system [77].

5. Conclusions

- Investigated resin-composites demonstrated a different shrinkage behavior that is strongly related to the different monomer and filler systems. The nature of the material determines the amount of the polymerization strain and its rate and the resultant stress.
- The results for the bulk-fill materials were within the lower range of the polymerization strain and stress with an exception of V-BF which showed high strain values.
- Flowable materials represented the higher range of the results in the polymerization stress and strain.
- Despite being a flowable material, GSO showed the highest elastic modulus compared to the other investigated materials.

REFERENCES

[1] Peutzfeldt A. Resin composites in dentistry: the monomer systems. Eur J Oral Sci 1997:97–116.
[2] Braga RR, Ballester RY, Ferracane JL. Factors involved in the development of polymerization shrinkage stress in resin-composites: a systematic review. Dent Mater 2005;21:962–70.
[3] Hilton TJ. Can modern restorative procedures and materials reliably seal cavities? In vitro investigations. Part 1. Am J Dent 2002;15:198–210.
[4] Bowen RL. Adhesive bonding of various materials to hard tooth tissues. VI. Forces developing in direct-filling materials during hardening. J Am Dent Assoc 1967;74:439–45.
[5] Bowen RL, Nemoto K, Rapson JE. Adhesive bonding of various materials to hard tooth tissues: forces developing in composite-materials during hardening. J Am Dent Assoc 1983;106:475–7.
[6] Gonçalves F, Pfeifer CS, Ferracane JL, Braga RR. Contraction stress determinants in dimethacrylate composites. J Dent Res 2008;87:367–71.
[7] Braga RR, Ferracane JL, Condon JR. Polymerization contraction stress in dual-cure cements and its effect on interfacial integrity of bonded inlays. J Dent 2002;30:333–40.
[8] Feilzer AJ, De Gee AJ, Davidson CL. Curing contraction of composites and glass-ionomer cements. J Prosthet Dent 1988;59:297–300.
[9] Stansbury JW, Trujillo-Lemon M, Lu H, Ding X, Lin Y, Ge J. Conversion-dependent shrinkage stress and strain in dental resins and composites. Dent Mater 2005;21:56–67.
[10] Davidson CL, De Gee AJ. Relaxation of polymerization contraction stresses by flow in dental composites. J Dent Res 1984;63:146–8.
[11] Venhoven BAM, de Gee AJ, Davidson CL. Polymerization contraction and conversion of light-curing BisGMA-based methacrylate resins. Biomaterials 1993;14:871–5.
[12] Feilzer AJ, De Gee AJ, Davidson CL. Quantitative determination of stress reduction by flow in composite restorations. Dent Mater 1990;6:167–71.
[13] Labella R, Lambrechts P, Van Meerbeek B, Vanherle G. Polymerization shrinkage and elasticity of flowable composites and filled adhesives. Dent Mater 1999;15:128–37.
[14] Vaidyanathan J, Vaidyanathan TK. Flexural creep deformation and recovery in dental composites. J Dent 2001;29:545–51.
[15] Feilzer AJ, Dooren LH, de Gee AJ, Davidson CL. Influence of light intensity on polymerization shrinkage and integrity of restoration-cavity interface. Eur J Oral Sci 1995;103:322–6.
[16] Kinomoto Y, Torii M, Takeshige F, Ebisu S. Comparison of polymerization contraction stresses between self- and light-curing composites. J Dent 1999;27:383–9.
[17] Feilzer AJ, De Gee AJ, Davidson CL. Setting stresses in composites for two different curing modes. Dent Mater 1993;9:2–5.
[18] Bouschlicher MR, Rueggeberg FA. Effect of ramped light intensity on polymerization force and conversion in a photoactivated composite. J Esthet Dent 2000; 12:328–39.
[19] Lim BS, Ferracane JL, Sakaguchi RL, Condon JR. Reduction of polymerization contraction stress for dental composites by two-step light-activation. Dent Mater 2002;18:436–44.
[20] Braga RR, Ferracane JL. Contraction stress related to degree of conversion and reaction kinetics. J Dent Res 2002;81: 114–8.
[21] Watts DC, Schneider LFJ, Marghalani HY. Bond-disruptive stresses generated by resin composite polymerization in dental cavities. J Adhes Sci Technol 2009;23:1023–42.
[22] Marchesi G, Breschi L, Antoniolli F, Di Lenarda R, Ferracane J, Cadenaro M. Contraction stress of low-shrinkage composite materials assessed with different testing systems. Dent Mater 2010;26:947–53.
[23] Stansbury JW. Synthesis and evaluation of novel multifunctional oligomers for dentistry. J Dent Res 1992;71:434–7.
[24] Craig RG, Powers JM. Restorative dental materials. 11th ed. St. Louis: Mosby; 2002.
[25] Barnes DM, Blank LW, Gingell JC, Gilner PP. A clinical evaluation of a resin-modified: glass ionomer restorative material. J Am Dent Assoc 1995;126:1245–53.
[26] Rueggeberg FA. From vulcanite to vinyl, a history of resins in restorative dentistry. J Prosthet Dent 2002;87:364–79.
[27] Kleverlaan CJ, Feilzer AJ. Polymerization shrinkage and contraction stress of dental resin composites. Dent Mater 2005;21:1150–7.
[28] Moszner N, Salz U. New developments of polymeric dental composites. Prog Polym Sci 2001;26:535–76.
[29] Mitra SB, Wu D, Holmes BN. An application of nanotechnology in advanced dental materials. J Am Dent Assoc 2003;134:1382–90.
[30] Turssi CP, Saad JRC, Duarte Jr SLL, Rodrigues Jr AL. Composite surfaces after finishing and polishing techniques. Am J Dent 2000;13:136–8.
[31] Chen MH, Chen CR, Hsu SH, Sun SP, Su WF. Low shrinkage light curable nanocomposite for dental restorative material. Dent Mater 2006;22:138–45.
[32] Trujillo-Lemon M, Ge J, Lu H, Tanaka J, Stansbury JW. Dimethacrylate derivatives of dimer acid. J Polym Sci Pol Chem 2006;44:3921–9.
[33] Ilie N, Hickel R. Investigations on a methacrylate-based flowable composite based on the SDR (™) technology. Dent Mater 2011;27:348–55.
[34] Kurokawa R, Finger WJ, Hoffmann M, Endo T, Kanehira M, Komatsu M, et al. Interactions of self-etch adhesives with resin composites. J Dent 2007;35:923–9.
[35] Ferracane JL. Resin composite – state of the art. Dent Mater 2011;27:29–38.
[36] Obici AC, Sinhoreti MAC, De Goes MF, Consani S, Sobrinho LC. Effect of the photo-activation method on polymerization shrinkage of restorative composites. Oper Dent 2002;27:192–8.

Please cite this article in press as: Al Sunbul H, et al. Polymerization shrinkage kinetics and shrinkage-stress in dental resin-composites. Dent Mater (2016), http://dx.doi.org/10.1016/j.dental.2016.05.006

[37] Watts DC, Marouf AS. Optimal specimen geometry in bonded-disk shrinkage-strain measurements on light-cured biomaterials. Dent Mater 2000;16:447–51.
[38] Watts DC, Marouf AS, Al-Hindi AM. Photo-polymerization shrinkage-stress kinetics in resin-composites: methods development. Dent Mater 2003;19:1–11.
[39] El-Damanhoury H, Platt J. Polymerization shrinkage stress kinetics and related properties of bulk-fill resin composites. Oper Dent 2014;39:374–82.
[40] Bandyopadhyay S. A study of the volumetric setting shrinkage of some dental materials. J Biomed Mater Res 1982;16:135–44.
[41] Fano V, Ma WY, Ortalli I, Pozela K. Study of dental materials by laser beam scanning. Biomaterials 1998;19:1541–5.
[42] Atai M, Watts DC, Atai Z. Shrinkage strain-rates of dental resin-monomer and composite systems. Biomaterials 2005;26:5015–20.
[43] Feilzer AJ, De Gee AJ, Davidson CL. Setting stress in composite resin in relation to configuration of the restoration. J Dent Res 1987;66:1636–9.
[44] Braga RR, Ferracane JL. Alternatives in polymerization contraction stress management. Crit Rev Oral Biol Med 2004;15:176–84.
[45] Yamamoto T, Ferracane JL, Sakaguchi RL, Swain MV. Calculation of contraction stresses in dental composites by analysis of crack propagation in the matrix surrounding a cavity. Dent Mater 2009;25:543–50.
[46] Tantbirojn D, Versluis A, Pintado MR, DeLong R, Douglas WH. Tooth deformation patterns in molars after composite restoration. Dent Mater 2004;20:535–42.
[47] Patel MP, Braden M, Davy KWM. Polymerization shrinkage of methacrylate esters. Biomaterials 1987;8:53–6.
[48] Venhoven BAM, De Gee AJ, Davidson CL. Light initiation of dental resins: dynamics of the polymerization. Biomaterials 1996;17:2313–8.
[49] Boaro LC, Gonçalves F, Guimarães TC, Ferracane JL, Pfeifer CS, Braga RR. Sorption, solubility, shrinkage and mechanical properties of "low-shrinkage" commercial resin composites. Dent Mater 2013;29:398–404.
[50] Sideridou ID, Karabela MM, Vouvoudi EC. Physical properties of current dental nanohybrid and nanofill light-cured resin composites. Dent Mater 2011;27:598–607.
[51] Sideridou I, Tserki V, Papanastasiou G. Effect of chemical structure on degree of conversion in light-cured dimethacrylate-based dental resins. Biomaterials 2002;23:1819–29.
[52] Dauvillier BS, Aarnts MP, Feilzer AJ. Modeling of the viscoelastic behavior of dental light-activated resin composites during curing. Dent Mater 2003;19:277–85.
[53] Feilzer AJ, Dauvillier BS. Effect of TEGDMA/BisGMA ratio on stress development and viscoelastic properties of experimental two-paste composites. J Dent Res 2003;82:824–8.
[54] Jang J-H, Park S-H, Hwang I-N. Polymerization shrinkage and depth of cure of bulk-fill resin composites and highly filled flowable resin. Oper Dent 2015;40:172–80.
[55] Watts DC, Cash AJ. Kinetic measurements of photo-polymerization contraction in resins and composites. Meas Sci Technol 1991;2:788–94.
[56] Hofmann N, Denner W, Hugo B, Klaiber B. The influence of plasma arc vs. halogen standard or soft-start irradiation on polymerization shrinkage kinetics of polymer matrix composites. J Dent 2003;31:383–93.
[57] Alvarez-Gayosso C, Barceló-Santana F, Guerrero-Ibarra J, Sáez-Espínola G, Canseco-Martínez MA. Calculation of contraction rates due to shrinkage in light-cured composites. Dent Mater 2004;20:228–35.
[58] Kannurpatti AR, Anderson KJ, Anseth JW, Bowman CN. Use of "living" radical polymerizations to study the structural evolution and properties of highly crosslinked polymer networks. J Polym Sci Pol Phys 1997;35:2297–307.
[59] Sabbagh J, Vreven J, Leloup G. Dynamic and static moduli of elasticity of resin-based materials. Dent Mater 2002;18:64–71.
[60] Watts DC. Elastic moduli and visco-elastic relaxation. J Dent 1994;22:154–8.
[61] Nakayama WT, Hall DR, Grenoble DE, Katz JL. Elastic properties of dental resin restorative materials. J Dent Res 1974;53:1121–6.
[62] El-Safty S, Silikas N, Akhtar R, Watts DC. Nanoindentation creep versus bulk compressive creep of dental resin-composites. Dent Mater 2012;28:1171–82.
[63] Beun S, Glorieux T, Devaux J, Vreven J, Leloup G. Characterization of nanofilled compared to universal and microfilled composites. Dent Mater 2007;23:51–9.
[64] Ikejima I, Nomoto R, McCabe JF. Shear punch strength and flexural strength of model composites with varying filler volume fraction, particle size and silanation. Dent Mater 2003;19:206–11.
[65] Braem M, Finger W, Van Doren VE, Lambrechts P, Vanherle G. Mechanical properties and filler fraction of dental composites. Dent Mater 1989;5:346–9.
[66] Soares CJ, Bicalho AA, Tantbirojn D, Versluis A. Polymerization shrinkage stresses in a premolar restored with different composite resins and different incremental techniques. J Adhes Dent 2013;15:341–50.
[67] Garoushi S, Vallittu PK, Lassila LVJ. Short glass fiber reinforced restorative composite resin with semi-inter penetrating polymer network matrix. Dent Mater 2007;23:1356–62.
[68] Garoushi S, Säilynoja E, Vallittu PK, Lassila L. Physical properties and depth of cure of a new short fiber reinforced composite. Dent Mater 2013;29:835–41.
[69] Stipho HD. Repair of acrylic resin denture base reinforced with glass fiber. J Prosthet Dent 1998;80:546–50.
[70] Vallittu PK. The effect of void space and polymerization time on transverse strength of acrylic-glass fibre composite. J Oral Rehab 1995;22:257–61.
[71] Lazaridou D, Belli R, Petschelt A, Lohbauer U. Are resin composites suitable replacements for amalgam? A study of two-body wear. Clin Oral Investig 2014:1–8.
[72] Sakaguchi RL, Peters MCRB, Nelson SR, Douglas WH, Poort HW. Effects of polymerization contraction in composite restorations. J Dent 1992;20:178–82.
[73] Feilzer AJ, de Gee AJ, Davidson CL. Relaxation of polymerization contraction shear stress by hygroscopic expansion. J Dent Res 1990;69:36–9.
[74] Braem M, Davidson CL, VanHerle G, Van Doren V, Lambrechts P. The relationship between test methodology and elastic behavior of composites. J Dent Res 1987;66:1036–9.
[75] Shah PK, Stansbury JW. Role of filler and functional group conversion in the evolution of properties in polymeric dental restoratives. Dent Mater 2014;30:586–93.
[76] Sideridou I, Tserki V, Papanastasiou G. Study of water sorption, solubility and modulus of elasticity of light-cured dimethacrylate-based dental resins. Biomaterials 2003;24:655–65.
[77] Asmussen E, Peutzfeldt A. Influence of UEDMA, BisGMA and TEGDMA on selected mechanical properties of experimental resin composites. Dent Mater 1998;14:51–6.

Please cite this article in press as: Al Sunbul H, et al. Polymerization shrinkage kinetics and shrinkage-stress in dental resin-composites. Dent Mater (2016), http://dx.doi.org/10.1016/j.dental.2016.05.006